Development of a therapeutic model of precancerous liver using crocin-coated magnetite nanoparticles

RKIA EL-KHARRAG[1,3], AMR AMIN[1], SOLEIMAN HISAINDEE[2], YASER GREISH[2] and SHERIF M. KARAM[3]

Departments of [1]Biology and [2]Chemistry, College of Science, [3]Department of Anatomy,
College of Medicine and Health Sciences, UAE University, Al-Ain, United Arab Emirates

Abstract. Despite considerable advances in understanding hepatocellular carcinoma, it is one of the common and deadliest cancers worldwide. Hence, increasing efforts are needed for early diagnosis and effective treatments. Saffron has been recently found to inhibit growth of liver cancer in rats. The aim of this study was to develop an effective method for treatment of liver cancer using magnetite nanoparticles (MNPs) coated with crocin, the main active component of saffron. MNPs were prepared and initially coated with dextran and a cross-linker to enhance conjugation of crocin using a modified coprecipitation method. Cultured HepG2 cells and diethylnitrosamine-injected mice were treated with corcin-coated MNPs and analyzed using cell proliferation assay and immunohistochemical analysis, respectively. Treatment of HepG2 cells with crocin-coated MNPs led to a significant inhibition of their growth as compared to control or those treated with free crocin or uncoated MNPs. Histological examinations of the livers of diethylnitrosamine-injected mice revealed several precancerous changes: multiple proliferative hepatic foci, hyper- or dysplastic transformations of bile ducts/ductules, and nuclear atypia associated with polyploidy, karyomegaly, and vacuolation. Immunohistochemistry using antibodies specific for cell proliferation (Ki-67) and apoptosis (M30-CytoDEATH and Bcl-2) revealed their upregulation during development of precancerous lesions. Using antibodies specific for inflammation (cyclooxygenase-2), oxidative stress (glutathione) and angiogenesis (vascular endothelial growth factor) indicated the involvement of multiple signaling pathways in the development of precancerous lesions. Treatment with crocin-coated MNPs was associated with regression of precancerous lesions, significant upregulation of apoptotic cells and downregulation of Bcl-2 labeling and markers of cell proliferation, inflammation, oxidative stress and angiogenesis. In conclusion, crocin-coated MNPs are more effective than free corcin for treatment of liver precancerous lesions in mice. These findings will help to develop new modalities for early detection and treatment of liver precancerous lesions.

Introduction

According to recent global statistics, liver cancer is the fifth most common cancer in men and the ninth in women. However, it is the second leading cause of cancer deaths in men and the sixth in women (1). More than 70% of the cases of primary liver cancer are hepatocellular carcinoma (2). It has approximately 8-month median survival without treatment which can be improved only by 3 months with the available chemotherapy (3). The primary side effects of most chemotherapeutic agents are their non-specificity and consequently cytotoxicity. Thus, the identification of new anticancer agents and use of enhanced drug delivery systems would increase specificity to cancer cells and reduce side effects of chemotherapy (4).

Natural products are commonly used for different purposes. Saffron, has been used in the treatment of some digestive and neoplastic disorders (5,6). Recent immunohistochemical and biochemical studies have demonstrated that saffron has significant therapeutic effects in a rat model of liver cancer through induction of apoptosis and downregulation of molecules involved in cellular proliferation, inflammation, and oxidative stress (7). Crocin is the main active component of saffron. It is a water-soluble carotenoid with antioxidant and anti-inflammatory properties (8). In addition, some studies have shown that crocin inhibits growth of different types of cancer cells derived from uterine cervix and mammary glands (9,10).

To enhance cancer therapy, the design of nanomaterials with specific functional properties that allow carrying therapeutic agents has become a promising approach (4). Magnetite nanoparticles (MNPs) are particularly useful drug carriers due

Correspondence to: Dr Sherif M. Karam, Department of Anatomy, College of Medicine and Health Sciences, UAE University, P.O. Box 17666, Al-Ain, United Arab Emirates
E-mail: skaram@uaeu.ac.ae

Dr Amr Amin, Department of Biology, College of Science, UAE University, P.O. Box 15551, Al-Ain, United Arab Emirates
E-mail: a.amin@uaeu.ac.ae

to their biocompatibility, biodegradability and superparamagnetic properties. Because of their large surface area-to-volume ratio, high quantity of anticancer agents can be loaded onto the surfaces of MNPs. When administered into patients, these therapeutic agents are released from MNPs at the cancer site by passive or active targeting, thereby offering the possibility of minimizing the side effects (11).

To improve their efficacy as drug carriers, MNPs can be initially coated with a natural polymer. Recently, monolithic and monodisperse MNPs have been produced using a modified coprecipitation method at low temperature (12). These MNPs can be subjected to surface functionalization using organic coatings, such as sodium dodecyl sulfate (13). In this study, the aims were first to prepare and characterize MNPs coated with dextran and crocin and then to test their effects on human hepatocellular carcinoma liver cancer cells *in vitro* and on a mouse model of liver carcinogenesis using diethylnitrosamine (DEN).

Materials and methods

Preparation of dextran-coated MNPs. Solutions containing 0.3 M of $FeCl_2\cdot 4H_2O$ and 0.6 M of $FeCl_3$ were prepared and injected into NaOH solutions containing 0.2, 0.5, 1.0 and 2.0% dextran with a feeding rate of 40 ml/h at 60˚C. When a brownish precipitate was formed, the solution was vigorously stirred for 1 h. Suspensions of dextran-coated MNPs were decanted and centrifuged at 3,000 rpm for 15 min followed by a successive decantation/washing with 25% ammonia solution. Dextran-coated MNPs were dried at 60˚C, finely ground, and characterized for their composition, morphology, thermal, and magnetic properties.

Benedict's test. To detect the unattached dextran in the coated MNPs solutions, Benedict reagent containing 0.8 M sodium citrate, 0.9 M sodium carbonate and 0.1 M copper sulfate were prepared in deionized water. Few drops of the mixed test solution were added to 2 ml of Benedict reagent and boiled for 5 min in a water bath. Formation of colored precipitate qualitatively indicated the presence of dextran in the solution.

Coating of MNPs with corcin. The concentration of 1% dextran coating for MNPs was chosen for further coating. To enhance crocin coating, a cross-linker molecule between dextran and crocin was added. Pre-calculated amounts of dextran-coated MNPs were suspended in autoclaved deionize water and completely dried. Succinic anhydride was added to dextran-MNPs in a ratio of 20:1 followed by N,N-dimethylacetamide (DMAc) as a solvent. The mixture was then stirred for 8 h at 90˚C in an oil bath. The remaining portion of MNPs coated with dextran and linker was washed three times with DMAc to remove unbound succinic anhydride. Each wash was followed by a centrifugation at 3,000 rpm for 15 min at room temperature and decantation. Freshly prepared 2 mmol 1-(3-dimethylaminopropyl)-3-ethylcarbodiimide hydrochloride in DMAc was added to MNPs coated with dextran and cross-linker and stirred at room temperature for 12 h under moisture-free conditions. Then, crocin at 50 or 100 mg/ml was added and stirred for 24 h at room temperature. Coated MNPs were centrifuged and washed with sterile deionized water 6 times at 4,000 rpm for 15 min. The resultant crocin-coated MNPs were precipitated and re-suspended in deionized water. UV-visible and Fourier transform infrared (FTIR) spectroscopic analyses were performed to confirm the presence of crocin on the surfaces of MNPs.

Characterization of crocin-coated MNPs. Crocin conjugation efficiency was determined by an indirect method involving detection of total free crocin concentration in the decanted solutions by measuring the absorbance at 440 nm (visible range) using a UV-visible spectrophotometer. The amounts of crocin coating on MNPs were calculated from the difference between the total amount of crocin initially used to coat MNPs and the amount of free crocin present in the decanted solutions (14).

The composition of MNPs was studied by FTIR spectroscopy using a Nicolet Nexus 470 infrared spectrophotometer (Thermo Fisher Scientific, Waltham, MA, USA). The FTIR spectra of the samples were recorded in solid state by KBr pellet method in the 400-4,000 cm^{-1} range. Thermogravimetric analysis was also carried out using a TGA-50 analyzer (Shimadzu, Kyoto, Japan), where the powder samples were heated to 600˚C at a rate of 20˚C/min using an aluminum pan. The percent weight loss was followed and correlated with the original composition of the MNPs. To visualize the crocin-coated MNPs, they were processed for imaging on carbon-coated copper grids by using Philips CM10 transmission electron microscopy (Eindhoven, The Netherlands).

Cell culture. HepG2 cells were obtained from the American Type Culture Collection (Manassas, VA, USA) and maintained in 75-cm^2 culture flasks using Dulbecco's modified Eagle's medium (DMEM), supplemented with 10% heat-inactivated fetal bovine serum (Sigma-Aldrich, St. Louis, MO, USA) and 1% penicillin/streptomycin (Sigma-Aldrich). Cells were grown in 5% CO_2 at 37˚C and 100% relative humidity. The culture medium was changed every 2 days and the cells were subcultured after 5-6 days using trypsin-EDTA (Sigma-Aldrich).

Methyl-thiazolyl-tetrazolium (MTT) assay. To determine the effective concentrations of crocin and MNPs, the MTT assay was used (15). Cells were seeded in 96-well plates at a density of 8,000 cells/well. After 24-h incubation, the culture medium was replaced with fresh medium containing free crocin (0.025, 0.05, 0.5, 3, 5, 8, 10, 15 or 20 mg/ml) or MNPs (0.05, 0.07, 0.09 or 0.1 mg Fe/ml). Then, the effects of 3 mg/ml crocin alone, 0.09 mg/ml total iron in MNPs alone, and 3 mg/ml crocin-coated MNPs on the cells were tested. After 72-h incubation, cells were washed with phosphate-buffered saline (PBS) and then 100 μl of fresh medium containing the tetrazolium dye, 3-(4,5-dimethylthiazol-2-Yl)-2,5-diphenyltetrazolium bromide at a final concentration of 5 mg/ml was added. Cells were then incubated at 37˚C for 1 h and the developed formazan product was solubilized by adding 100 μl of isopropanol for 30 min. The absorbance was measured at 560 nm using Perkin-Elmer spectrophotometer (Waltham, MA, USA). The percent viability of the treated cells was determined in relation to control cells cultured without any treatment.

Animals. Balb/c mice were obtained from the animal facility of the College of Medicine and Health Sciences, UAE University. Animals were housed under a 12-h light/dark cycle

each at 24-26˚C. They were maintained on standard laboratory animal diet with food and water *ad libitum*. All animal studies were carried out in accordance with and after approval of the Animal Research Ethics Committee of the College of Medicine and Health Sciences, UAE University.

Experimental design. To induce carcinogenesis, 3-week-old male Balb/c mice (n=12) were injected intraperitoneally with 50 mg/kg body weight of DEN twice a week for 8 weeks. Mice were randomly divided into three groups and injected through the tail vein twice a week for two weeks either by 100 µl of saline, or 11 mg/kg body weight crocin alone, or 11 mg/kg crocin-coated MNPs. The concentration of iron in the injected MNPs was 17 mg/kg body weight (0.3 mg Fe/100 µl). This dose was previously reported to be non-toxic (16). For control, untreated weight- and sex-matched normal littermate mice were used. Similar experimental groups of mice (n=12) were treated with double the dose of free crocin (22 mg/kg) or crocin-coated MNPs (22 mg/kg). In these mice, the concentration of iron in the injected MNPs was also 17 mg/kg body weight.

One day after the last injection, mice were weighed, anesthetized, and dissected. The livers were immediately removed, weighed, and examined for the presence of any visible lesions. The right lobes were fixed in 10% buffered formalin and processed for paraffin embedding. For comparison, four livers representing the different groups (control, DEN-induced, crocin-treated, crocin-coated MNPs-treated) were processed simultaneously and embedded together in the same paraffin block. Tissue blocks were serially sectioned at 5-micron thickness, stained with hematoxylin and eosin (H&E), and then examined using Olympus BX41 microscope (Olympus, Tokyo, Japan). Images were taken using DP70 digital camera. Adjacent sections were processed for Prussian blue staining and immunohistochemical analysis.

Prussian blue staining. To detect the presence of iron of the MNPs in liver tissues, tissue sections were deparaffinized, rehydrated and incubated for 35 min in an aqueous solution containing equal amounts of 20% hydrochloric acid and 10% potassium ferrocyanide mixed immediately before use. Tissues were counterstained with neutral red or H&E.

Immunohistochemical studies. Liver tissue sections were deparaffinized, rehydrated and washed in PBS. For antigen retrieval, tissue sections were incubated for 45 min in 10 mM citrate buffer at pH 6.0 and heated at 98˚C. To inhibit endogenous peroxidase activity, sections were incubated in 3% hydrogen peroxide in methanol for 1 h at room temperature. To ensure similar conditions to all tissue sections, tissues of the different groups were encircled with PAP pen (Sigma-Aldrich) and exposed together to the same solutions. Tissues were blocked in 1% bovine serum albumin containing 0.5% Tween-20 in PBS for 45 min. Sections were then incubated for 1 h at room temperature or overnight at 4˚C with rabbit polyclonal antibodies specific for: Ki-67 (Abcam, Cambridge, MA, USA), M30-CytoDEATH (Roche, Penzberg, Germany), Bcl-2 (Abcam), glutathione S-transferase Pi (GST; Medical and Biological Laboratories Co., Ltd., Nagoya, Japan), cyclooxygenase-2 (COX-2; Abcam) and vascular endothelial growth factor (VEGF; Abcam).

Following a PBS wash, the avidin-biotin-peroxidase complex method was used. Tissue sections were incubated with biotinylated anti-rabbit antibodies (Jackson ImmunoResearch, West Grove, PA, USA) for 2 h. Extravidine peroxidase conjugate (Sigma-Aldrich) was added for 1 h. The antigen-antibody binding sites were revealed by using 3,3'-diaminobenzidine (Sigma-Aldrich). Some of the tissues were counterstained with hematoxylin.

Quantification of protein expression in tissue sections. To provide a quantitative evaluation for the expression of the different biomarkers in tissue sections, digital images were processed using Image-Pro software version 6.0 for Windows. The percentage (%) of immunolabeled area per image taken at a final magnification of x400 was estimated. A total of 20 different images per probed tissue section were analyzed for each group of the mice.

Statistical analysis. The quantification data of MTT assay and immunohistochemistry were represented as mean ± standard error of the means. The mean values were compared using GraphPad Prism software (La Jolla, CA, USA) for Windows and the one-way analysis of variance (ANOVA) with Tukey post hoc procedure. Results were considered significant at values of $P<0.05$, moderately significant at $P<0.01$, and highly significant at $P<0.001$.

Results

Properties of MNPs. MNPs prepared by using a modified coprecipitation method at low temperature were coated *in situ* with dextran and crocin as summarized in Fig. 1A. These MNPs possessed a good dispersibility and stability in water and spherical shape with uniform size of 16 nm average diameter (Fig. 1B). Thermogravimetric analysis confirmed the presence of dextran on MNPs and helped to determine its optimal concentration. Pure MNPs showed an average weight loss of 14% due to removal of water that was physically adsorbed onto their surfaces (Fig. 2A). Pure dextran showed an initial weight loss of 10% at 100-150˚C due to water removal followed by a major weight loss of 92% at 300˚C due to combustion of dextran and degradation of polysaccharide chains. Increasing concentrations of dextran on MNPs showed a similar pattern as pure dextran confirming the presence of dextran on their surfaces. Dextran concentration of 1% was optimal to use because higher concentration was not associated with any significant increase in weight loss (Fig. 2B).

FTIR spectra of pure crocin showed bands at 1,515 and 1,631 cm^{-1} (due to C=C bond), 1,697 cm^{-1} (C=O bond), and 2,933 cm^{-1} (C-H bond). The broad stretch between 3,262 and 3,441 cm^{-1} corresponded to the presence of OH group (Fig. 2C). This pattern was in line with previously described FTIR analysis (17). FTIR spectrum of crocin-coated MNPs showed the unique bands of C=C at 1,534 and 1,637 cm^{-1} which was only present in crocin, confirming the successful coating of MNPs with crocin (Fig. 2C).

Effects of crocin treatments on the viability of HepG2 cells. Treatments of HepG2 cells with increasing concentrations of crocin (from 0.025 to 20 mg/ml) revealed a reduction in cellular
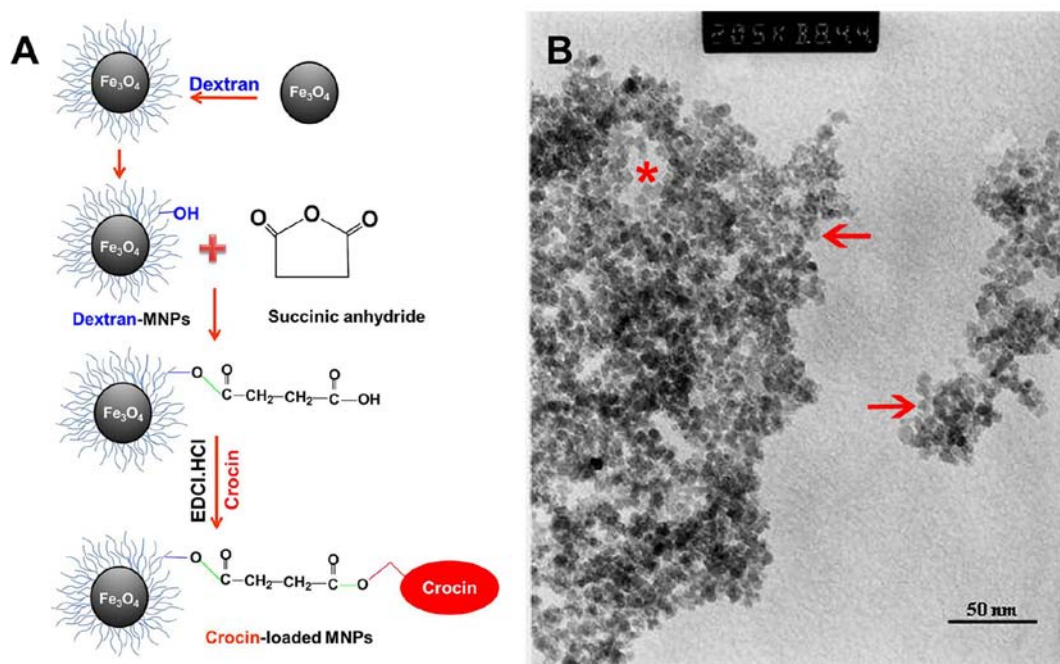
Figure 1. Preparation, characterization, and effects of crocin-coated MNPs. (A) Schematic presentation of the coating process of MNPs (Fe_3O_4) with dextran, cross-linker (succinic anhydride) and crocin. (B) Transmission electron micrograph of MNPs prepared by coprecipitation method showing their homogeneous spherical shape, as can be seen around the asterisk and at the arrows. Scale bar, 50 nm.
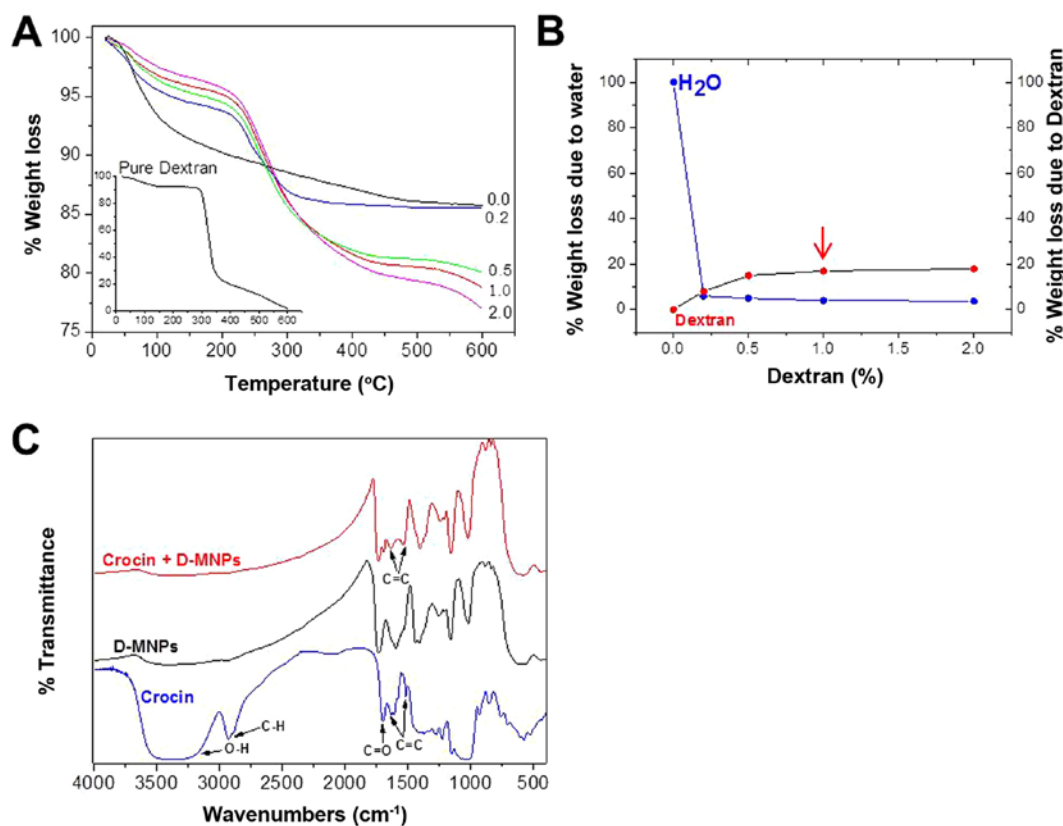

Figure 2. Characterization of MNPs. (A) Thermogravimetric analysis (TGA) of MNPs coated with various concentrations of dextran. The inset shows the TGA pattern of pure dextran. (B) The effect of dextran coating on the extent of decomposition of the coating contents with temperature. Data are derived from the TGA in (A). (C) FTIR spectra of MNPs coated with dextran and crocin (Crocin + D-MNPs), MNPs coated with dextran (D-MNPs), and free crocin.

density in the culture plate starting from 3 mg/ml concentration. These changes were confirmed by MTT assay (Fig. 3A).

Incubation of HepG2 cells with crocin revealed a gradual reduction in cellular viability starting from the concentration
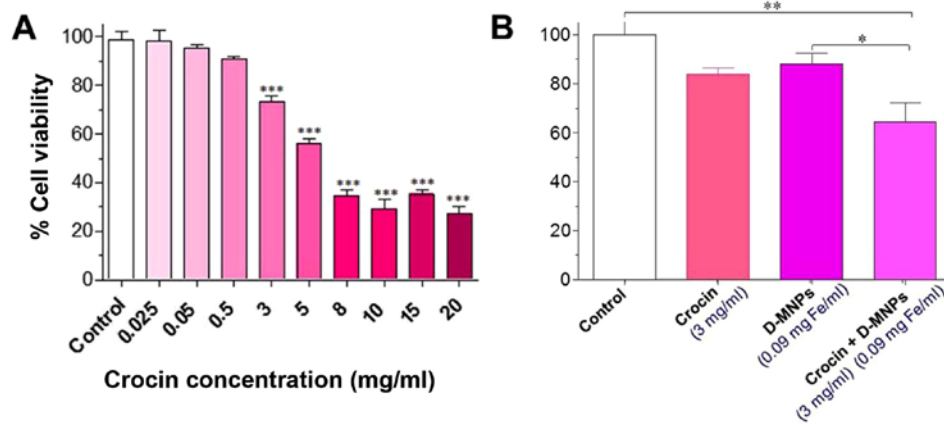
Figure 3. MTT assay using HepG2 cells treated for 72 h with: (A) different concentrations of free crocin (0.025-20 mg/ml) and (B) free crocin, MNPs coated with dextran, and MNPs coated with dextran and crocin. Values are expressed as mean ± SEM. $^{*}P \leq 0.05$, $^{**}P \leq 0.01$, $^{***}P \leq 0.001$.
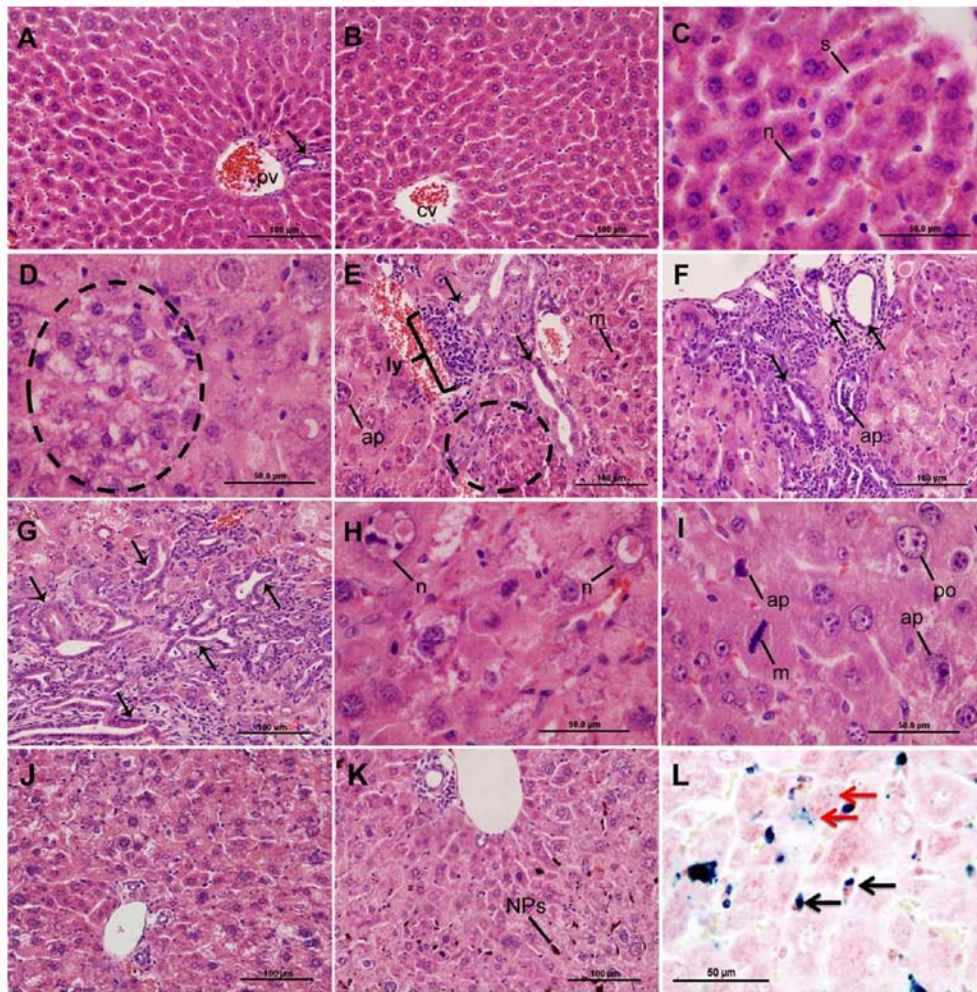

Figure 4. Microscopic analysis of liver tissue sections obtained from normal mice (A-C) and mice injected with DEN (D-I), DEN and free crocin (J) and DEN and crocin-coated D-MNPs (K and L). Tissues were stained with H&E (A-K) and Prussian blue (L). Normal liver tissues demonstrate: (A) portal area with a branch of the pv, a bile duct (arrow), and radiating numerous plates of acidophilic hepatocytes, (B) central vein (cv) surrounded by numerous plates of hepatocytes, (C) hepatocytes which appear polyhedral, mono- and bi-nucleated (n), and separated by interconnected sinusoids (s). DEN-injected liver tissues demonstrate different signs of precancerous changes: (D) pale hepatocellular foci (dashed circle) made of lightly stained hepatocytes, (E) dark hepatocellular foci (dashed circle) of small hepatocytes, aggregations of small lymphoid cells (ly), multiple profiles of bile ducts (arrows), and scattered mitotic (m) and apoptotic cells (ap), (F) hyperplastic bile ducts which may acquire dilated lumen (arrows) with apoptotic dark cells (ap), (G) numerous dysplastic bile ducts (arrows) with disrupted architecture, (H) nuclear atypia and some nuclei appear huge with vacuolar spaces (n), and (I) nuclear po with m and ap cells. Liver tissues of mice injected with DEN and then treated with 11 mg/kg crocin: (J) free crocin induces an improvement in the overall architecture of the liver tissue and the portal area appears in the lower left side, (K) crocin-coated D-MNPs also induces an improvement in the liver tissue with a normal portal area seen at the top. The brownish structures indicate the NPs. (L) Prussian blue staining to demonstrate the accumulation of MNPs in the hepatocytes (red arrows) and Kupffer cells (black arrows) of liver tissue of a mouse treated with crocin-coated D-MNPs. Scale bar, 100 (A, B, E-G, J and K) and 50 μm (C, D, H, I and L).

Table I. The percentages of areas immunolabeled with antibodies specific for different biomarkers in the livers of normal mice and mice injected with DEN, DEN plus crocin, and DEN plus crocin-coated D-MNPs.[a]

Biomarkers	Conc.	% Immunolabeled areas (mean ± SEM)			
		Normal	DEN	DEN + Crocin	DEN + Crocin-D-MNPs
Ki-67	L	0.19±0.03	1.20±0.13	0.97±0.10	0.83±0.09
	H	0.10±0.01	1.16±0.08	0.85±0.08	0.43±0.03
M30	L	0.06±0.01	0.48±0.05	0.79±0.09	0.87±0.08
	H	0.21±0.03	0.88±0.10	1.24±0.15	1.56±0.12
Bcl-2	L	3.38±0.49	22.23±1.53	17.96±2.92	13.80±2.45
	H	8.98±1.39	33.53±3.0	20.54±2.29	17.02±1.85
GST	L	0.44±0.08	6.63±1.56	2.52±0.48	2.54±0.27
	H	1.83±0.20	14.29±1.91	9.46±1.01	7.24±0.78
COX-2	L	9.21±0.56	39.70±2.28	32.26±1.78	21.13±2.06
	H	7.74±0.61	46.37±1.80	30.40±2.12	18.18±1.52
VEGF	L	5.59±0.61	48.21±4.27	43.70±4.24	39.04±3.98
	H	6.51±1.12	52.45±2.47	39.85±3.00	29.53±2.72

[a]Data are presented for low (L) and high (H) concentrations (11 and 22 mg/kg body weight, respectively) of crocin (free or conjugated to D-MNPs).

of 3 mg/ml in a dose-dependent manner. It reached ~70% at a dose of 3 mg/ml when compared with control and became 55% at a dose of 5 mg/ml (Fig. 3A). The effect of MNPs on the viability of HepG2 cells was also tested. Increasing concentrations of iron in the media for 72 h showed a decrease in cell viability starting from 0.07 mg/ml. There was no significant effect at 0.05 mg/ml compared to the control (data not shown). Based on these data and published information on the dose of MNPs (18), it was decided to use crocin-coated MNPs containing 3 mg crocin and 0.09 mg iron per ml. The effects of such amounts of crocin and iron either alone or conjugated were tested on HepG2 cells. The data revealed that crocin alone reduced the percentage of viable cells as compared to control. This reduction was significantly (P<0.01) enhanced when crocin-coated MNPs were used (Fig. 3B).

Effects of crocin treatments on the histological features of the livers. Tissue sections of normal control liver showed the usual pattern of lobules with peripheral portal areas including small bile ducts/ductules (Fig. 4A-C). The administration of DEN into mice caused several histopathological signs: i) multiple pale or basophilic hepatocellular foci (Fig. 4D and E), ii) lymphocytic infiltrations and hyperplastic or dysplastic changes (Fig. 4E-G), iii) hepatocytes with nuclear atypia or pleomorphism, karyomegaly, polyploidy, and vacuolation (Fig. 4D, H and I), iv) prominent apoptotic cells (Fig. 4E and F), and v) increased mitotic figures in portal areas and hepatocytes (Fig. 4E and I).

Treatment of DEN-injected mice with free crocin or crocin-coated D-MNPs induced apparent recovery of liver histology (Fig. 4J). This effect was more apparent in mice treated with crocin-coated D-MNPs (Fig. 4K). The presence of crocin-coated D-MNPs in the liver tissues was demonstrated by Prussian blue staining (Fig. 4L). Variable accumulations of blue-stained MNPs were observed in the cytoplasm of hepatocytes and some scattered interstitial cells, probably phagocytic Kupffer cells (Fig. 4L).

Effects of crocin treatments on cell proliferation. To investigate cell division in the livers of control and treated mice, immunohistochemistry using anti-Ki-67 antibodies was applied. Immunolabeled cells were very few in the livers of normal mice (Fig. 5A), but were apparent and numerous after DEN injection (Fig. 5B). While these dividing cells were mainly found in the walls of amplifying bile ducts/ductules in the portal areas, some were hepatocytes and interstitial/lymphoid cells. Cell proliferation was also apparent in hepatocellular foci, made of numerous small compact hepatocytes. Quantifications revealed >6-fold increase in the areas of Ki-67 immunoreactivity in DEN-injected mice (Table I). This significant hyperproliferation was slightly reduced in mice treated with 11 and 22 mg/kg free crocin (Fig. 5C, E and F). The percent decrease was estimated at 20 and 27, respectively. This reduction was significantly enhanced when mice were treated with similar doses of crocin but conjugated to MNPs (Fig. 5D-F). So, the percent decrease of cell proliferation reached 31 and 62, respectively (Table I).

Effects of crocin treatments on apoptosis. Immunolocalizations of M30 epitope of the cleaved cytokeratin 18 in normal livers showed no or an occasional positively labeled cell (Fig. 6A). In DEN-injected mice, there was a consistent cytoplasmic labeling, but only in a few scattered cells (Fig. 6B). These M30-positive cells became even more apparent in mice treated with crocin (Fig. 6C) and crocin-coated D-MNPs (Fig. 6D). Quantifications revealed that the percent increase in cell death with crocin-coated D-MNPs was highly significant (P≤0.001) when compared with the values of DEN-injected mice (Fig. 6E and F and Table I).

When the anti-apoptotic Bcl-2 protein was investigated, no immunolabeling was detected in normal liver cells (Fig. 7A). However, the immunolocalization of Bcl-2 was apparent in
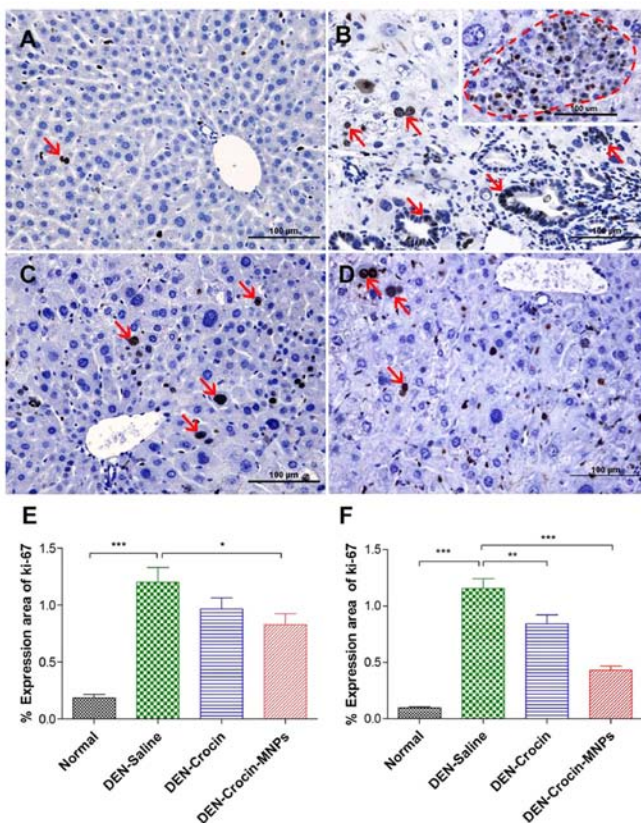
Figure 5. Immunohistochemical analysis of Ki-67. Labeling is demonstrated in normal (A), DEN-injected (B), free crocin-treated (C), and crocin-coated D-MNPs-treated (D) mice. In these representative mouse tissue sections, the dose of free and conjugated crocin was similar, 11 mg/kg body weight. (A) In normal mouse tissue, Ki-67-labeled cells are very few (arrow). (B) In DEN-injected tissue, there is a massive increase in Ki-67-labeled cells (arrows). These dividing cells are mainly found in the wall of the hyperplastic bile ducts (lower three arrows), hepatocytes (upper 2 arrows), and the hepatocellular foci (dashed oval area in the inset). (C) In free crocin-treated tissue, the Ki-67-positive cells are reduced (arrows). (D) In tissue treated with crocin-coated D-MNPs, there are only a few Ki-67-labeled cells (arrows). The scattered dark brown structures are aggregated D-MNPs. Scale bar, 100 μm. The graphs demonstrate the quantifications of the percent of Ki-67 labeled areas in normal and DEN-injected mice as compared to mice treated with 11 (E) or 22 mg/kg (F) of free crocin or D-MNPs coated with crocin. Note that the level of Ki-67-labeling in normal mice is very low, but highly increased in DEN injected mice. Treatments with crocin (free or conjugated to D-MNPs) reduced the expression area of Ki-67 and is highly significant when the high dose of crocin-coated D-MNPs was used. Values are expressed as mean ± SEM; $^*P \leq 0.05$, $^{**}P \leq 0.01$, $^{***}P \leq 0.001$.
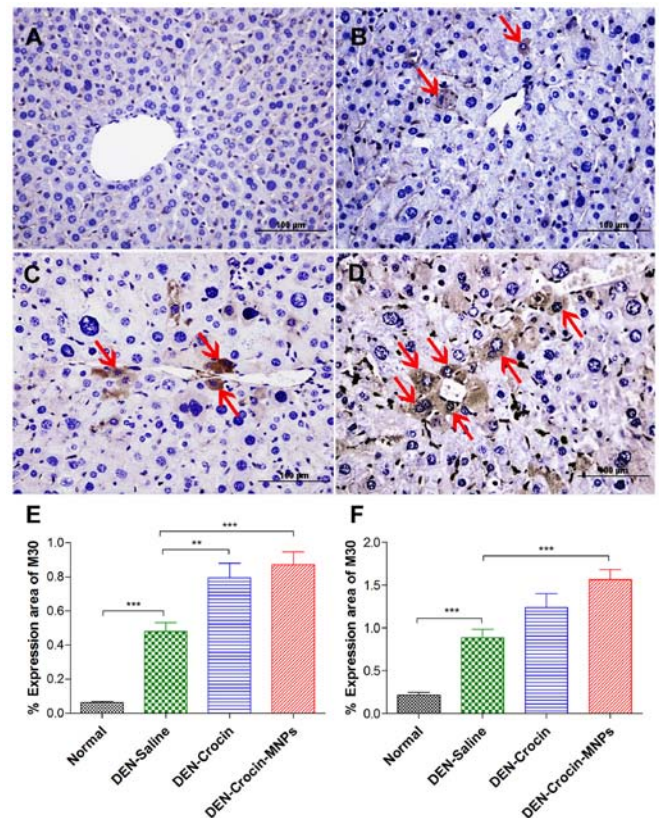
Figure 6. Immunohistochemical analysis of caspase-cleaved cytokeratin 18 using M30-CytoDEATH antibody in liver tissues of normal (A) DEN-injected (B), free crocin-treated (C), and crocin-coated D-MNPs-treated (D) mice. The dose of free and conjugated crocin was similar, 11 mg/kg body weight. (A) In normal mouse tissue, M30 immunolabeling appears negative. (B) In DEN-injected tissue, a few M30-positive cells (arrows) are present. (C) In free crocin-treated tissue, the M30-positive cells are apparent (arrows). (D) In tissue treated with crocin-coated D-MNPs, there are many M30-positive hepatocytes (arrows). Scale bar, 100 μm. Quantification of the percent of M30 expression areas in normal and DEN-injected mice as compared to mice treated with 11 (E) or 22 mg/kg (F) free crocin or crocin-coated with D-MNPs. Note that the percent area of M30-positive cells in normal groups is very low and highly increased in DEN-injected mice. Treatments with crocin (free or conjugated to D-MNPs) enhanced the M30 labeling to become highly significant when the high dose of crocin-coated D-MNPs is used. Values are expressed as mean ± SEM; $^{**}P \leq 0.01$, $^{***}P \leq 0.001$.

DEN-injected mice as compared to any of the other groups of mice (Fig. 7B-D). The immunostaining was specifically cytoplasmic. The expression of Bcl-2 in liver tissues of mice treated with crocin-coated D-MNPs was reduced as compared to DEN-injected or free crocin-treated mice. Quantifications confirmed the microscopic observations and showed significant differences between the levels of Bcl-2 expression in mice treated with 11 and 22 mg/kg crocin-coated D-MNPs as compared to those of DEN-injected mice (Fig. 7E and F and Table I).

Effects of crocin treatments on GST immunolabeling. Microscopic examination of normal liver tissues probed with anti-GST antibodies revealed no or occasional cells expressing GST (Fig. 8A). However, many hepatocytes were positively stained for GST in DEN-induced mice (Fig. 8B). The staining was homogeneously cytoplasmic with some variations in the

intensity and distribution. Abnormal hepatocytes with large vacuolated nuclei were more intensely stained than other surrounding cells with normal morphology. In these altered cells, the nuclei were also labeled with anti-GST antibody (Fig. 8B). In DEN-injected mice treated with 11 mg/kg of crocin, there was a decrease in the staining for GST (Fig. 8C). This reduction in GST immunolabeling was more apparent in mice treated with crocin-coated MNPs (Fig. 8D).

Quantifications revealed an increase by ≥16-fold in the percent areas of GST immunolabeling in DEN-induced mice when compared with normal mice (Fig. 8E and Table I). However, the percentages of areas labelled with GST in mice treated with 11 and 22 mg/kg of free or coated crocin on D-MNPs were significantly decreased as compared with those of DEN-injected mice (Fig. 8E and F and Table I).

Effects of crocin treatments on COX-2 immunolabeling. In normal mice, COX-2 immunoreactivity was weak in normal liver tissues (Fig. 9A). In DEN-injected mice, there was an
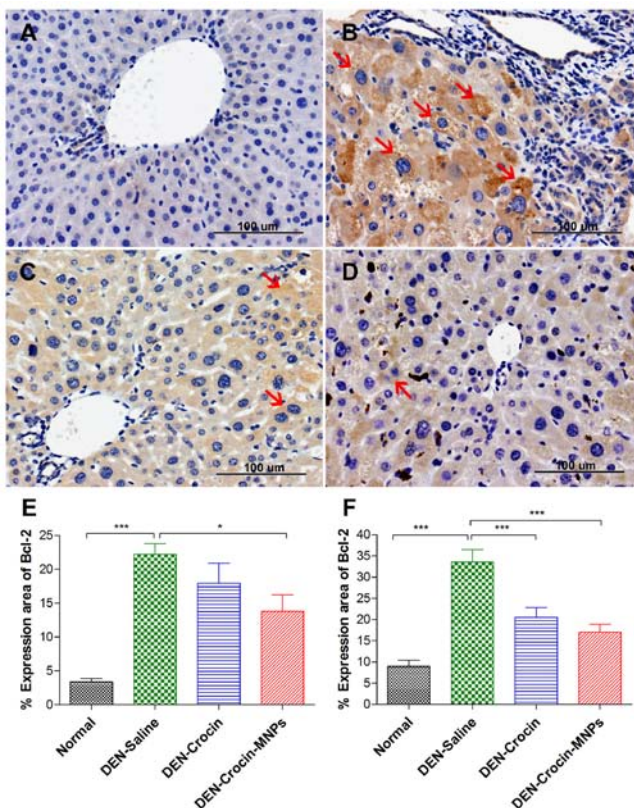
Figure 7. Immunohistochemical analysis of Bcl-2 labeling in liver tissues of normal (A), DEN-injected (B), free crocin-treated (C), and crocin-coated D-MNPs-treated (D) mice. In these representative mouse tissue sections, the dose of free and conjugated crocin was similar, 11 mg/kg body weight. (A) In normal mouse tissue, there are very few or no Bcl-2-labeled cells. (B) In DEN-injected tissue, there is a massive increase in Bcl-2-labeled cells (arrows). (C) In free crocin-treated tissue, the Bcl-2-positive cells are reduced (arrows). (D) In tissue treated with crocin-coated D-MNPs, there are only a few Ki-67-labeled cells (arrows). Scale bar, 100 μm. The graphs demonstrate the quantification of the percent of Bcl-2-labeled areas in normal and DEN-injected mice as compared to mice treated with 11 (E) or 22 mg/kg (F) of free crocin or D-MNPs coated with crocin. Note that the level of Bcl-2-labeling in normal mice is very low, but highly increased in DEN injected mice. Treatments with crocin (free or conjugated to D-MNPs) reduced the expression area of Bcl-2 and is highly significant when the high dose of crocin-coated D-MNPs is used. Values are expressed as mean ± SEM; *P≤0.05, **P≤0.01, ***P≤0.001.
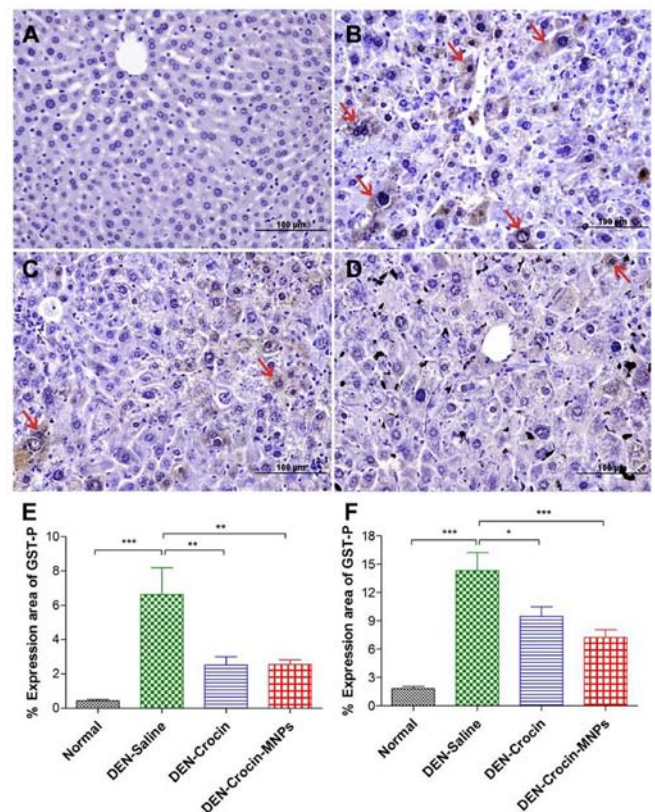

Figure 8. Immunohistochemical analysis of GST labeling in liver tissues of normal (A), DEN-injected (B), free crocin-treated (C), and crocin-coated D-MNPs-treated (D) mice. The dose of free and conjugated crocin was similar, 11 mg/kg body weight. (A) In normal mouse tissue, GST immunolabeling appears negative. (B) In DEN-injected tissue, hepatocytes with GST-positive cells (arrows) are apparent. (C) In free crocin-treated tissue, the GST-positive cells are few and barely seen (arrows). (D) In tissue treated with crocin-coated D-MNPs, there are very few (arrow) or no GST-positive hepatocytes. The scattered dark brown structures are the aggregated D-MNPs. Scale bar, 100 μm. Quantification of the percent of GST expression areas in normal and DEN-injected mice as compared to mice treated with 11 (E) or 22 mg/kg (F) free crocin or crocin-coated with D-MNPs. Note that the expression of GST in normal groups was very low and highly increased in DEN injected mice. Treatments with crocin (free or conjugated to D-MNPs) reduced the expression area of GST and is highly significant when the high dose of crocin-coated D-MNPs were used. Values are expressed as mean ± SEM; *P≤0.05, **P≤0.01, ***P≤0.001.

apparent COX-2 immunolabeling (Fig. 9B). COX-2 expression was localized in the cytoplasm of hepatocytes around both the central vein and portal areas. Quantification revealed that COX-2 expression was significantly increased by >4-fold in DEN-injected mice compared to normal mice (Fig. 9E and F). However, COX-2 was significantly reduced (P≤0.001) in the liver tissues treated with 11 or 22 mg/kg crocin-coated D-MNPs compared with DEN-injected or free crocin-treated mice (Fig. 9C-F).

Effects of crocin treatments on VEGF immunolabeling. VEGF immunoreactivity was very week in normal mice, but a strong cytoplasmic expression was found in DEN-injected mice (Fig. 10A and B). Moreover, VEGF expression was inhibited after the treatment with free crocin or with crocin-coated D-MNPs (Fig. 10C and D). Measurements of the areas stained for VEGF showed that their significant (P<0.001) increase in DEN-injected mice was ≥8-fold (Fig. 10E and F). Whereas the inhibition of VEGF immunostaining was not significant when

low dose of free or conjugated crocin was used. It became significant only when the crocin dose was doubled (Fig. 10E and F and Table I).

Discussion

Drug delivery via MNPs utilizes their multifunctional properties and the distinctive characteristics of cancer tissue, such as leaky vasculature (19). In this study, MNPs were prepared using a modified coprecipitation method. To reduce their aggregation, they were first coated with dextran, a natural polysaccharide polymer known for its biocompatibility (20). The overall size of MNPs must be sufficiently small to evade rapid filtration by the spleen but large enough to avoid renal clearance. MNPs >100 nm are sequestered by phagocytosis, while particles smaller than 10 nm are rapidly removed though renal clearance (11). So, the 16-nm size of crocin-coated D-MNPs produced in this study are suitable for drug delivery.
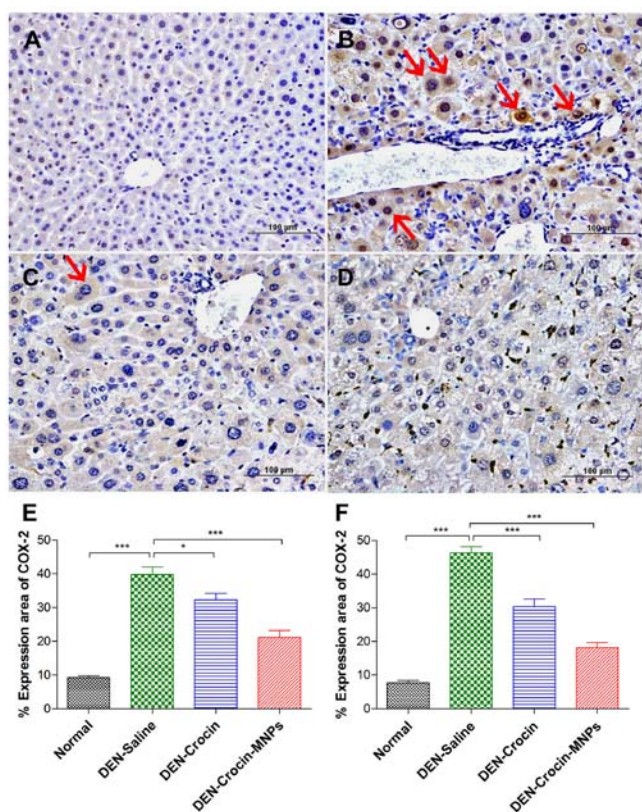
Figure 9. Immunohistochemical analysis of Cox-2 labeling in liver tissues of normal (A), DEN-injected (B), free crocin-treated (C), and crocin-coated D-MNP-treated (D) mice. In these representative mouse tissue sections, the dose of free and conjugated crocin was similar, 11 mg/kg body weight. (A) In normal mouse tissue, there are very few or no Cox-2-labeled cells. (B) In DEN-injected tissue, there are numerous Cox-2-labeled cells (arrows). (C) In free crocin-treated tissue, the Cox-2-positive cells are reduced (arrows). (D) In tissue treated with crocin-coated D-MNPs, there are only a few or no Cox-2-labeled cells. Scale bar, 100 μm. The graphs demonstrate the quantifications of the percent of Cox-2-labeled areas in normal and DEN-injected mice as compared to mice treated with 11 (E) or 22 mg/kg (F) of free crocin or D-MNPs coated with crocin. Note that the level of Cox-2-labeling in normal mice is very low, but highly increased in DEN injected mice. Treatments with crocin (free or conjugated to D-MNPs) reduced the expression area of Cox-2 and is highly significant when the low or high doses of crocin-coated D-MNPs are used. Values are expressed as mean ± SEM; $^{*}P \leq 0.05$, $^{**}P \leq 0.01$, $^{***}P \leq 0.001$.
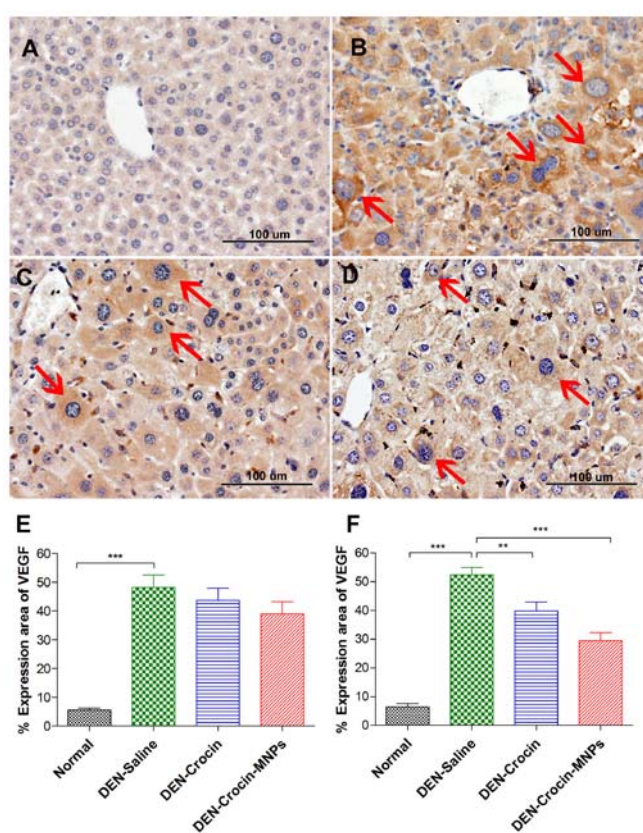

Figure 10. Immunohistochemical analysis of VEGF labeling in mouse liver tissues. (A) In normal tissue, there are no VEGF-labeled cells. (B) In DEN-injected tissue, there are numerous VEGF-labeled hepatocytes (arrows). (C) In free crocin-treated tissue, the VEGF-labelled cells are reduced (arrows) in number and intensity. (D) In liver tissue treated with crocin-coated D-MNPs, there are only a few VEGF-labeled cells. In (C) and (D), the dose of free and conjugated crocin was similar, 11 mg/kg body weight. Scale bar, 100 μm. The graphs demonstrate the percent of VEGF-labeled areas in normal and DEN-injected mice as compared to mice treated with 11 (E) or 22 mg/kg (F) of crocin (free or or conjugated to D-MNPs). Note that the difference between VEGF-labeling in normal and DEN-injected mice is highly significant. Treatment with crocin (free or conjugated to D-MNPs) reduced the expression area of VEGF and becomes significant when high doses of free or conjugated crocin are used. Values are expressed as mean ± SEM; $^{**}P \leq 0.01$, $^{***}P \leq 0.001$.

Crocin is a water-soluble carotenoid with significant anti-cancer effects (21,22). In this study, MTT assay showed that crocin also inhibits growth of HepG2 cells in a dose-dependent manner. Several mechanisms were proposed for the action of crocin involving effects on cell proliferation and apoptosis (21,22). However, crocin was found to have no toxic effects on normal cells such as human skin fibroblasts (22).

HepG2 cells incubated with different iron concentrations in dextran-conjugated MNPs showed good biocompatibility due to their dextran coating. The slight decrease in cell viability might be because some MNPs lost their dextran coating, consequently exposing iron to the cells. Similarly, it was demonstrated that iron used at 0.01-0.1 mg/ml was safe for growth of MCF-7 cells (18). Accordingly, in this study, the biocompatible dextran-conjugated MNPs containing 0.09 mg/ml iron were coated with crocin for *in vitro* and *in vivo* studies. When HepG2 cells were incubated with crocin and dextran-coated MNPs containing 3 mg/ml crocin and 0.09 mg/ml Fe, there was a reduction in cell count due to the

release and interaction of crocin with the cells. The effect of crocin-coated MNPs was more pronounced than that of free crocin possibly due to: i) gradual release of crocin leading to prolonged time of interaction, and ii) enhanced delivery of crocin-coated D-MNPs to the cells by different mechanisms such as adsorption and endocytosis (23).

The carcinogenic effect of DEN could be due to different mechanisms: i) alkylating DNA structures leading to the formation of mutagenic DNA adducts, ii) generating ROS that damages DNA, protein, and lipid molecules, iii) inducing mutations in H-ras proto-oncogene leading to unlimited cell division, iv) inducing overexpression of the Bcl-2 gene, and v) stimulating the proliferation of hepatic oval cells and bile duct cells leading to hyperplasia and the formation of microscopic precancerous lesions (24,25).

Multiple injections of DEN were found to induce preneoplastic changes in young mice probably in two stages: initially by enhancing apoptosis and then, DNA synthesis is stimulated and ultimately precancerous lesions are formed. This model also mimics the human conditions in which cycles of degeneration
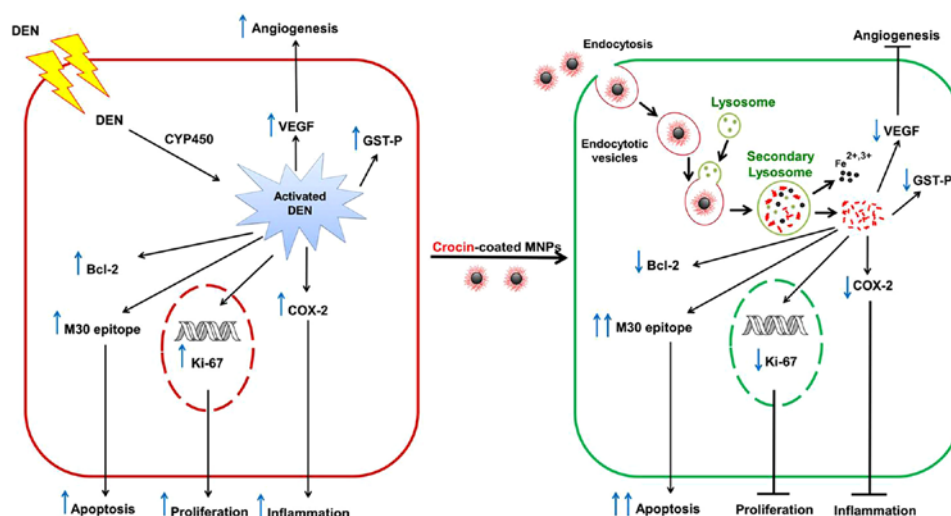
Figure 11. Diagrammatic representation summarizing the effects of DEN on liver cells and demonstrating the consequences of treatment with conjugated crocin.

and regeneration might activate preneoplastic transformations. The younger the mice, the faster cancer will develop because of the high proliferation rates in young animals. Male mice were used in this study due to the stimulating effect of androgens and the inhibitory effect of estrogens on hepatocarcinogenesis (26).

Apoptosis is essential for tissue homeostasis and also plays a role in carcinogenesis (27). During apoptosis, the mitochondrial outer membrane becomes permeable and releases multiple proteins into the cytosol leading to activation of caspases and cleavage of different substrates including cytokeratin 18. In this study, M30 localization in DEN-injected mice showed an increased apoptotic cells which might have contributed to the increased cell proliferation to replace dead cells. Saffron treatment was found to increase the number of M30 positive cells in DEN-injected rats (7). This study demonstrates that the numbers of M30-positive apoptotic cells are increased in mice treated with crocin-coated D-MNPs compared to DEN-injected or free crocin-treated mice (Fig. 6).

Bcl-2 is known to prolong cellular survival by blocking apoptosis induced by a wide variety of death signals (27). This study shows that Bcl-2 is highly expressed in DEN-injected mice. This is in line with previous studies on DEN-induced tumors in the mouse liver with upregulation of Bcl-2 (28). In this study, the inhibitory effect of crocin on Bcl-2 expression was significantly enhanced when it was conjugated with D-MNPs (Fig. 7).

Previous studies revealed that GST induction occurs in pre-neoplastic cell populations (29). In this study, the expression of GST protein was significantly upregulated in liver tissues of DEN-injected mice compared to normal mice. Treatment with crocin-coated D-MNPs is associated with decreased pre-cancerous lesions and a significant downregulation of GST expression. Therefore, GST appears to be a good marker to follow progression and regression of hepatic preneoplastic lesions.

COX-2 overexpression is associated with an increase in prostaglandin levels which affects many mechanisms involved in carcinogenesis, such as angiogenesis, inhibition of apoptosis, stimulation of cell growth and invasiveness of tumor cells (30,31). Therefore, COX-2 is an important molecular target for anticancer therapies. Its expression is undetectable

in most normal tissues and is highly induced in the livers of DEN-injected rats (32). Similar results were reported in this study. Dietary feeding with crocin for 4 weeks was able to inhibit colonic adenocarcinomas in mice and decrease the mRNA expression of inflammation regulators such as COX-2 (33). Therefore, free crocin has a role in inhibiting COX-2 expression in animals with cancer, which explains the reduction in COX-2 expression in crocin-treated animals. Moreover, this effect was increased in 11 and 22 mg/kg crocin-coated D-MNPs-treated mice, indicating the role of D-MNPs in improving the anticancer activity of crocin.

VEGF plays critical roles in tumor angiogenesis, invasion and metastasis, and vascular permeability (34). The expression of VEGF induced by DEN injections was decreased with 11 and 22 mg/kg crocin that was attached to MNPs compared to free crocin treated group, indicating the enhancement of anticancer effect of crocin upon loading it on MNPs.

The use of MNPs as a carrier system for crocin delivery is very promising for cancer therapy due to several reasons. The nano-size of the magnetite particles is well tolerated by the organism. When injected into animals, they degrade with time into products that can be re-used by the body cells. They have high surface area to volume ratio that allows them to upload high amount of crocin onto their surfaces. MNPs are able to deliver crocin in the precancerous tissues by passive targeting due to enhanced permeability and retention effect. The stability of crocin is enhanced by its conjugation onto the surfaces of MNPs. While free crocin has low stability and its functionality is reduced by exposure to heat, oxygen, or light, MNPs preserve crocin in its intact active form (35). The concentrations of crocin and MNPs used in this study were non-toxic and the used crocin-coated MNPs were monodispersed and stable in several solutions including water, DMEM and saline.

In conclusion, this study demonstrates that MNPs enhance anticancer effects of crocin and improve its biological effects using *in vitro* (HepG2 cells) and *in vivo* (liver preneoplastic lesions) models. Immunohistochemical analysis demonstrated the involvement of different cellular pathways in the development of precancerous liver and demonstrated their possible use as prognostic recovery markers in mice treated with

free crocin or crocin-coated D-MNPs. Since the hepatocytes undergo a slow renewal process it is anticipated that there will be a complete but slow recovery of the liver tissue when the treatment is discontinued. A proposed mechanism for the effects of crocin-coated MNPs is depicted in Fig. 11. Crocin released from D-MNPs inhibits cell proliferation and stimulates caspase-mediated apoptosis. The anti-inflammatory and anti-angiogenesis effects of crocin are demonstrated by downregulation of COX-2 and VEGF. Therefore, the functionalized D-MNPs are useful tools for delivery of crocin to enhance its anticancer effects. These results could help in designing new modalities for early detection and treatment of liver precancerous lesions to hopefully reduce the high incidence and mortality rate of hepatocellular carcinoma.

Acknowledgements

References

1. Torre LA, Bray F, Siegel RL, Ferlay J, Lortet-Tieulent J and Jemal A: Global cancer statistics, 2012. CA Cancer J Clin 65: 87-108, 2015.
2. London W and McGlynn K: Liver cancer. In: Cancer Epidemiology and Prevention. 3rd edition. Schottenfeld D and Fraumeni JF (eds). Oxford University Press, New York, NY, pp763-786, 2006.
3. Llovet JM, Ricci S, Mazzaferro V, Hilgard P, Gane E, Blanc JF, de Oliveira AC, Santoro A, Raoul JL, Forner A, et al; SHARP Investigators Study Group: Sorafenib in advanced hepatocellular carcinoma. N Engl J Med 359: 378-390, 2008.
4. Tietze R, Zaloga J, Unterweger H, Lyer S, Friedrich RP, Janko C, Pöttler M, Dürr S and Alexiou C: Magnetic nanoparticle-based drug delivery for cancer therapy. Biochem Biophys Res Commun 468: 463-470, 2015.
5. Block KI, Gyllenhaal C, Lowe L, Amedei A, Amin AR, Amin A, Aquilano K, Arbiser J, Arreola A, Arzumanyan A, et al: Designing a broad-spectrum integrative approach for cancer prevention and treatment. Semin Cancer Biol 35 (Suppl): S276-S304, 2015.
6. Kianbakht S and Mozaffari K: Effects of saffron and its active constituents, crocin and safranal on prevention of indomethacin induced gastric ulcers in diabetic and nondiabetic rats. J Med Plants 8: 30-38, 2009.
7. Amin A, Hamza AA, Bajbouj K, Ashraf SS and Daoud S: Saffron: A potential candidate for a novel anticancer drug against hepatocellular carcinoma. Hepatology 54: 857-867, 2011.
8. Tamaddonfard E, Farshid AA, Eghdami K, Samadi F and Erfanparast A: Comparison of the effects of crocin, safranal and diclofenac on local inflammation and inflammatory pain responses induced by carrageenan in rats. Pharmacol Rep 65: 1272-1280, 2013.
9. Khosrojerdi F and Kazemi Noureini S: Study of telomerase activity in cell line MCF7 treated with crocin. Clin Biochem 44: S113, 2011.
10. Escribano J, Alonso GL, Coca-Prados M and Fernández JA: Crocin, safranal and picrocrocin from saffron (Crocus sativus L.) inhibit the growth of human cancer cells in vitro. Cancer Lett 100: 23-30, 1996.
11. Singh A and Sahoo SK: Magnetic nanoparticles: A novel platform for cancer theranostics. Drug Discov Today 19: 474-481, 2014.
12. El-kharrag R, Amin A and Greish YE: Low temperature synthesis of monolithic mesoporous magnetite nanoparticles. Ceram Int 38: 627-634, 2012.
13. El-kharrag R, Amin A and Greish YE: Synthesis and characterization of mesoporous sodium dodecyl sulfate-coated magnetite nanoparticles. J Ceram Sci Tech 2: 203-210, 2011.
14. Sundar S, Mariappan R and Piraman S: Synthesis and characterization of amine modified magnetite nanoparticles as carriers of curcumin-anticancer drug. Powder Technol 266: 321-328, 2014.
15. Mosmann T: Rapid colorimetric assay for cellular growth and survival: Application to proliferation and cytotoxicity assays. J Immunol Methods 65: 55-63, 1983.
16. Mejías R, Pérez-Yagüe S, Gutiérrez L, Cabrera LI, Spada R, Acedo P, Serna CJ, Lázaro FJ, Villanueva A, Morales MP, et al: Dimercaptosuccinic acid-coated magnetite nanoparticles for magnetically guided in vivo delivery of interferon gamma for cancer immunotherapy. Biomaterials 32: 2938-2952, 2011.
17. Dar RA, Brahaman PK, Tiwari S and Pitre KS: Indirect electrochemical analysis of crocin in phytochemical sample. E-J Chem 9: 918-925, 2012.
18. Kumar SR, Priyatharshni S, Babu VN, Mangalaraj D, Viswanathan C, Kannan S and Ponpandian N: Quercetin conjugated superparamagnetic magnetite nanoparticles for in-vitro analysis of breast cancer cell lines for chemotherapy applications. J Colloid Interface Sci 436: 234-242, 2014.
19. Dawidczyk CM, Kim C, Park JH, Russell LM, Lee KH, Pomper MG and Searson PC: State-of-the-art in design rules for drug delivery platforms: Lessons learned from FDA-approved nanomedicines. J Control Release 187: 133-144, 2014.
20. Molday RS and MacKenzie D: Immunospecific ferromagnetic iron-dextran reagents for the labeling and magnetic separation of cells. J Immunol Methods 52: 353-367, 1982.
21. Amin A, Bajbouj K, Koch A, Gandesiri M and Schneider-Stock R: Defective autophagosome formation in p53-null colorectal cancer reinforces crocin-induced apoptosis. Int J Mol Sci 16: 1544-1561, 2015.
22. Aung HH, Wang CZ, Ni M, Fishbein A, Mehendale SR, Xie JT, Shoyama CY and Yuan CS: Crocin from Crocus sativus possesses significant anti-proliferation effects on human colorectal cancer cells. Exp Oncol 29: 175-180, 2007.
23. Veiseh O, Gunn JW and Zhang M: Design and fabrication of magnetic nanoparticles for targeted drug delivery and imaging. Adv Drug Deliv Rev 62: 284-304, 2010.
24. Rumsby PC, Barrass NC, Phillimore HE and Evans JG: Analysis of the Ha-ras oncogene in C3H/He mouse liver tumours derived spontaneously or induced with diethylnitrosamine or phenobarbitone. Carcinogenesis 12: 2331-2336, 1991.
25. He XY, Smith GJ, Enno A and Nicholson RC: Short-term diethylnitrosamine-induced oval cell responses in three strains of mice. Pathology 26: 154-160, 1994.
26. Nakatani T, Roy G, Fujimoto N, Asahara T and Ito A: Sex hormone dependency of diethylnitrosamine-induced liver tumors in mice and chemoprevention by leuprorelin. Jpn J Cancer Res 92: 249-256, 2001.
27. Lowe SW and Lin AW: Apoptosis in cancer. Carcinogenesis 21: 485-495, 2000.
28. Lee GH: Correlation between Bcl-2 expression and histopathology in diethylnitrosamine-induced mouse hepatocellular tumors. Am J Pathol 151: 957-961, 1997.
29. Satoh K, Kitahara A, Soma Y, Inaba Y, Hatayama I and Sato K: Purification, induction, and distribution of placental glutathione transferase: A new marker enzyme for preneoplastic cells in the rat chemical hepatocarcinogenesis. Proc Natl Acad Sci USA 82: 3964-3968, 1985.
30. Gallo O, Franchi A, Magnelli L, Sardi I, Vannacci A, Boddi V, Chiarugi V and Masini E: Cyclooxygenase-2 pathway correlates with VEGF expression in head and neck cancer. Implications for tumor angiogenesis and metastasis. Neoplasia 3: 53-61, 2001.
31. Tang TC, Poon RT, Lau CP, Xie D and Fan ST: Tumor cyclooxygenase-2 levels correlate with tumor invasiveness in human hepatocellular carcinoma. World J Gastroenterol 11: 1896-1902, 2005.
32. Sivaramakrishnan V and Niranjali Devaraj S: Morin regulates the expression of NF-kappaB-p65, COX-2 and matrix metalloproteinases in diethylnitrosamine induced rat hepatocellular carcinoma. Chem Biol Interact 180: 353-359, 2009.
33. Kawabata K, Tung NH, Shoyama Y, Sugie S, Mori T and Tanaka T: Dietary crocin inhibits colitis and colitis-associated colorectal carcinogenesis in male ICR mice. Evid Based Complement Alternat Med 2012; 820415, 2012.
34. Lee SH, Jeong D, Han YS and Baek MJ: Pivotal role of vascular endothelial growth factor pathway in tumor angiogenesis. Ann Surg Treat Res 89: 1-8, 2015.
35. Maggi L, Carmona M, Zalacain A, Tomé MM, Murcia MA and Alonso GL: Parabens as agents for improving crocetin esters' shelf-life in aqueous saffron extracts. Molecules 14: 1160-1170, 2009.